An Experimental Study of Quasi-Synchronous Multiuser Communications in Cluttered Scenarios at Low VHF

Fikadu T. Dagefu, $Member, IEEE$, Gunjan Verma, Predrag Spasojevic, $Member, IEEE$, and Brian M. Sadler, $Fellow, IEEE$

***Abstract*—Reliable, ad hoc communication among multiple users is a crucial objective in complex tactical scenarios. A major challenge is that synchronization mechanisms (such as GPS) are intermittent and fixed centralized coordinators (e.g., base stations) are infeasible. Classical approaches to multiuser communications relying on tight time synchronization and/or power control are impractical in such scenarios. Furthermore, state-of-the-art systems operating at microwave frequencies suffer from lack of penetration and multipath effects causing significant channel variability and exacerbating the near-far effect. In this paper, we investigate the potential advantages of the favorable channel characteristics of the lower VHF band for reliable multiuser communications in highly cluttered environments among near ground nodes. We focus on a class of code division multiple access (CDMA) strategies known as quasi-synchronous (QS) direct sequence (DS) CDMA and use moderate to high QAM constellations. A key aspect of QS CDMA codes is their robustness to coarse inter-user time synchrony and power mismatch, which greatly relaxes the rate that nodes must re-synchronize with each other. Our study experimentally explores the possibilities of multiuser communications in harsh environments among near-ground nodes. Our measurements involve three canonic indoor-to-outdoor, indoor-to-indoor and through-building channels characterized by obstacles and clutter that represent very difficult propagation environments, especially at microwave frequencies. We also study the spatial and temporal variability of our system and characterize the impact of frequency offset on code orthogonality with simulations and experiments. We show that our system has strong potential for excellent multiuser performance in infrastructure-poor regimes.**

***Index Terms*—Multiuser communications, lower VHF, quasi-synchronous CDMA, mobile ad-hoc networking, Spectral efficiency**

I. Introduction

Agile mobile ad-hoc networks are fundamental enablers for tactical military and civilian applications such as emergency response and disaster rescue. In such applications, the goal is to achieve reliable communications among near-ground mobile nodes forming ad-hoc topologies, moving about in cluttered scenes, and consuming low power. Conventional approaches achieve this goal by using coordinating wired infrastructure combined with elevated base stations, which provides time, frequency, and power synchronization among all nodes. On the other hand, to maximize the utility of tactical networks, it is highly desirable to minimize reliance on such coordinating infrastructure while enabling moderate data rates. The problem is that without such infrastructure, classical approaches suffer an unacceptable loss in multiuser performance.

Even in the presence of coordinating infrastructure, near-ground mobile nodes operating in cluttered scenes and at conventional microwave frequencies often have uncertain and highly variable performance. This is due to significant signal attenuation, multipath, and short coherence times that require costly hardware and signal processing solutions to partially mitigate.

By contrast, recent studies show that lower frequencies (i.e., upper HF and lower VHF bands) have favorable near-ground propagation characteristics including reduced multipath, superior penetration, and increased channel coherence time. This translates into sufficient signal-to-noise ratio (SNR) for many communications applications even with very low power transmission in complex propagation environments [1]-[2]. The large size and low efficiency of conventional low frequency antennas has historically been a major bottleneck for practical applications; however, recent development of miniature antennas having moderate gain has enhanced their practical utility [3]-[7] and reinvigorated the potential for near-ground mobile communications and geolocation applications at lower VHF [8]-[12].

In this paper, we design and experimentally study a reduced-infrastructure low-power mobile ad-hoc network communication paradigm at low VHF. Conventional systems require chip level time synchronization amongst base stations/users [18]. It may be very challenging for ad hoc nodes to achieve this level of synchrony; conversely, operation having a reduced level of synchrony leads to loss of orthogonality and near-far problems which require coordinated power control. Our approach is based on quasi-synchronous (QS) direct sequence code division multiple access (DS-CDMA) in which codes are spread in time and are characterized by their zero cross-correlation zone (ZCZ) [19].

In addition to coarse time synchrony, ad-hoc nodes suffer from coarse frequency synchrony due to oscillator frequency offset as well as Doppler shift. This induces loss of code orthogonality and a resulting degradation in multiuser performance. Compared to systems at microwave frequencies, the effects of frequency offset are significantly reduced at lower VHF. This is because both oscillator as well as Doppler induced frequency offsets increase at higher frequencies. Correspondingly, we here illustrate that our approach is robust to realistic frequency offsets found at lower VHF.

Previous research has characterized various aspects of the QS-DS-CDMA system [13]-[15]. In [14], various design

strategies for code families with a ZCZ property were presented. The effect of carrier frequency offset (CFO) were investigated on a variety of code families including Gold and Walsh codes in DS-CDMA systems [15]. This study, however, did not include codes with a ZCZ. In [16], we show that such a system when combined with multiple sub-carriers can greatly reduce time synchronization requirements; e.g., enabling nodes to time-synchronize approximately once every $20s$, rather than once per second as required in conventional systems. We consider the multi-carrier extension in other work.

We focus on characterizing performance of a low VHF QS-DS-CDMA system having low-infrastructure requirements in very difficult cluttered indoor-outdoor scenarios based on simulations and experiments. We first study the performance of the developed codes via simulations by introducing known imperfections including inter-user delays and frequency offsets. We then conduct experiments in several canonical indoor and outdoor scenarios that include significant power mismatches caused by near-far scenarios, as well as propagation in the presence of multiple metal reinforced walls and floors. We achieve excellent M-QAM communications performance in these scenarios (we have tested up to 256-QAM); our results highlight five important aspects. One, even though we use simple receiver processing (e.g., no multiuser detection or RAKE combining) we still achieve high signal-to-interference-plus-noise ratio (SINR) measures indicating minimal multiple-access and intersymbol interference (MAI,ISI). This liberates nodes from using complex, power-hungry signal processing. Two, we find spatial and temporal stability of the signal of interest when the interference signal's delay falls inside the ZCZ. This suggests that training symbols (for channel estimation/equalization) can be sent infrequently, reducing communication overhead. Three, we find that even when the interferer is near the receiver, the signal of interest is minimally affected. This liberates the system designer from employing power control mechanisms. Four, we find high SINRs even when using very high order modulations, e.g. up to 256-QAM. This illustrates the possibility for achieving high spectral efficiencies. Five, we study the effect of induced frequency offset (even beyond the typical offsets expected at lower VHF) on the interference suppression of the QS-DS-CDMA. Our results show that multiuser performance is minimally affected due to frequency offsets realistically present in systems operating at low VHF.

The rest of this paper is organized as follows. In Section II, we summarize the details of the QS-DS-CDMA system including its time/frequency synchronization tradeoff. In Section III, we show simulation results. In Section IV, we describe our measurement system and experiment scenarios. In Section V, we illustrate the experimental performance of the proposed approach based on measurements in complex propgation channels.

II. Overview of the QS-DS-CDMA System

In this section we outline the QS-DS-CDMA approach and describe relevant system parameters for the specific design utilized in this paper. All users operate in a shared bandwidth w_t. Each user communicates at a rate of R symbols per second and uses one of K codes of length L. The codes are designed so as to ensure the existence of a zero correlation zone (ZCZ) in which the signal is immune to inter-symbol and multiple access interference. ZCZ is a design parameter measured in chips; the largest delay (in chips) still within the ZCZ is denoted Z. As long as the delay between users is less than or equal to Z, their cross-correlation is guaranteed to be zero. Let Δt be the maximum time offset between nodes in seconds.

The ZCZ code design bound states that $K < L/Z$ (see for example [14]), so that maximizing the number of users for a given bandwidth and rate implies that the ZCZ length should be minimized.

Let Δf_0 be the target maximum *design* frequency offset among interfering signals at the receiver and C be a constant that is a function of the ZCZ code design. Unless the frequency offset $\Delta f_0 < C \cdot R$, it may induce a significant loss of orthogonality and hence, interference, even when the inter-user delay is less than or equal to Z chips.

In this paper we study loosely synchronized (LS) family of ZCZ codes from [14] transmitted over a single-carrier with a center frequency of 40MHz. As an example we consider a family size of 16 LS codes with a ZCZ $Z = 3$ and length $L = 70$ (base code of length 64 plus 6 zero padding chips). The signal bandwidth is $w_t = 1.25$ MHz, communication (symbol) rate is $R = 17.86$ KSyms/sec (71.4 Kbps for 16-QAM, 107.2 Kbps for 64-QAM, 142.9 Kbps for 256-QAM) and chip duration $t_c = 1/w_t = .8\mu s$. Hence, the maximum interference-free time uncertainty is $\Delta t < Z \cdot t_c = 2.4\mu s$; the design frequency offset uncertainty is $\Delta f_0 < CR = C \cdot 19.6kHz = 352$Hz (for $C = .02$ which is empirically estimated). The Software Defined Radios (SDR) used for experiments at lower VHF have frequency offsets less than 20 Hz. Our current setup is overdesigned for frequency offset which will be useful in the multi-carrier extension of the single carrier work in this paper in which the sensitivity to frequency offset grows with the number of carriers.

III. Simulation Based Analysis

In this section, we present simulation results based on the spreading codes described in the previous section. The simulations serve as a baseline analysis to understand the performance of the codes by introducing various imperfections such as frequency offset, inter-user delay, and transmit power variation among the users, which emulates the well known near-far problem. The relevant simulation system parameters are included in the previous section. Fifteen transmitters are treated as interferers having varying delays, frequency offsets and transmit power levels and are assumed to be at equal distance from the receiver of interest as depicted in Figure 1. In our experiments described next, LS preambles are used to achieve synchronization between the receiver and transmitters.

In Figure 2 example simulation results for a 16-QAM constellation are shown. For a given point in the x-axis (i.e., maximum delay in chips t_d), each user is assigned a random relative delay between 0 and t_d. The users are assigned random phase offsets. The frequency offset for each user is also randomly selected between 0 and Δf_0 where Δf_0

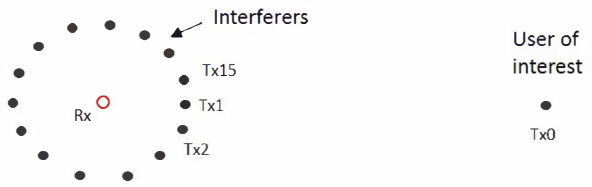

Fig. 1. Tx-Rx simulation configuration.

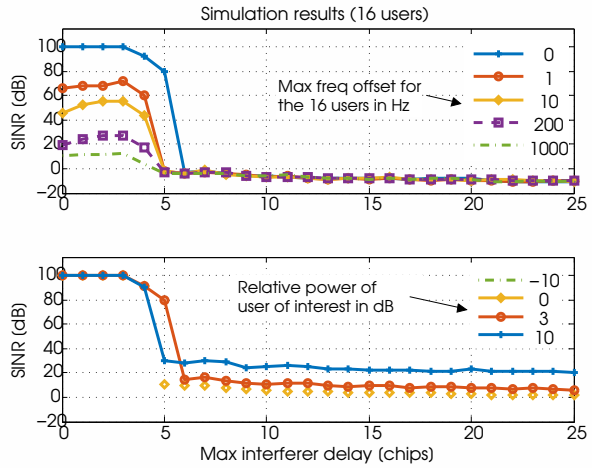

Fig. 2. A simulation scenario where 15 interferers (with varying relative power levels and frequency offsets) are positioned around the receiver and one transmitter of interest is positioned at a varying distance from the receiver. In the top plot, the SINR vs delay in chips is provided where the curves are parameterized by Δf_0, with random frequency offset in the range $[0, \Delta f_0]$ is assigned to the users. In the bottom plot, the SINR vs delay in chips is provided where the various curves correspond to the power of the link of interest relative to interferer's received power.

is varied for each simulation. Each data point is computed by running 100 realizations of the parameters and taking the mean. The top plot in Figure 2 shows the SINR vs delay in chips where the various curves correspond to the maximum frequency offset Δf_0. It can be seen that, even in the presence of frequency offset (up to 10s of Hz), high SINR is achieved within the ZCZ. The radios utilized in our experiments, which will be described in the next sections, have a maximum frequency offset of 20 Hz. In the bottom plot, the SINR vs delay in chips is provided where the various curves correspond to the relative transmit power of the user of interest. It can be seen that very high SINR is achieved within the ZCZ even when the link of interest has much smaller received power compared to the interferer's power at the receiver, which is the result of high interference rejection that the designed codes provide. The sections that follow focus on experimentally characterizing the performance of the proposed multiuser communications paradigm in complex non-line-of-sight (NLoS) scenarios.

IV. Experiments in Complex Scenarios

In this section, we detail our experimental setup, measurement parameters, and measurement scenarios.

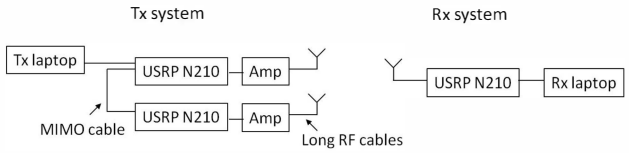

Fig. 3. The experimental testbed configuration, with two transmit and one receive USRP. The Tx USRPs are wired to enable programmable offsets, and the Tx antennas are spread using lengthy RF cables.

A. Experimental Setup

We develop an SDR testbed and utilize it with compact low VHF antennas to carry out experiments in realistic indoor and outdoor environments. In addition to realistic experiments, our testbed allows us to study the effects of various levels of imperfections in a controlled way (such as level of synchronization, frequency offset or power mismatch between users). As shown in Figure 3, the transmitter and receiver systems utilize the Universal Radio Software Peripheral (USRP) model N210 SDR. The USRP N210 consists of an FPGA, a 100 MS/s ADC, a 400 MS/s DAC, and a modular daughtercard. We use the BasicTx and BasicRx daughtercards. The QS-DS-CDMA system parameters are given in Section II.

The antennas used for these experiments are $\lambda/6$ short dipoles having a 3dB impedance bandwidth of 3 MHz with a center frequency of 40 MHz. It should be noted that we have an ongoing research effort where highly miniaturized low frequency antennas have been developed enabling the integration of the radios and antennas on small ground robotic platforms [4]-[5]. In all measurements, the phase center of the transmit and receive antennas is 70 cm above ground. The peak transmit power used in the measurements range from 30 to 200 milliwatts. The results presented in this paper focus on a three node system where two nodes are transmitters and the third is the receiver. One of the two transmitters, which we denote user 2, is declared the user of interest, while the other, user 1, is the interferer. Low noise amplifiers and narrow passband filters are also utilized. The two transmitters are connected via a cable and associated software which enables precisely controllable time/frequency coordination between the nodes. The existence of this coordination allows us to induce various known delays and/or frequency offsets between the two transmitters in software. This controlled experimental setup allows us to systematically study the limits of the proposed technique with different levels of known degraded synchronization.

B. Measurement Scenarios

Measurements are conducted in NLoS indoor/outdoor and through-building channels. All measurements are carried out in and around a large, highly cluttered five story office building that has extensive metal partitions and reinforcement. The measurement scenarios are described below (see Figure 6 and Table I).

- Scenario 1 consists of a receiver positioned in a courtyard near the building, one transmitter (user 1 considered as the interferer) is moved around the receiver and a second

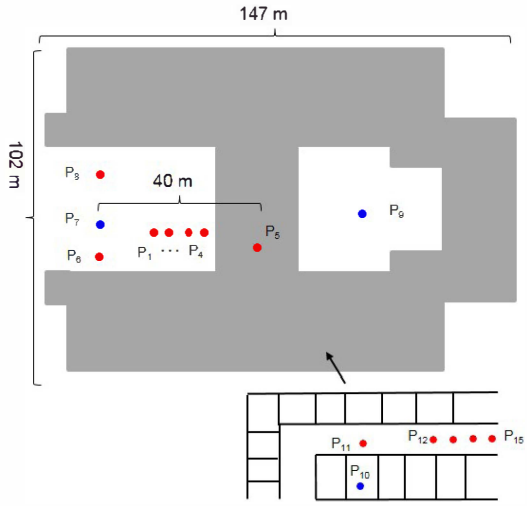

Fig. 4. The measurements were carried out in and around a large five story building. NLoS indoor/outdoor and through-building channels are considered (see Table I).

transmitter (user 2) is positioned inside the first floor of the building $40m$ from the receiver.

- Scenario 2 consists of a receiver and one transmitter (interferer) located near the receiver and the second transmitter (user 2) located in the hallway. Measurements are taken in the hallways, adjacent to offices and large interior lab bays (for various locations of user 2). The distance between the measured points and the receiver ranges from 20m to 50m.
- Scenario 3 focuses on measurements through the building where the two transmitters are positioned at ground level on one side of the building and the receiver is located on the other side in a courtyard which is the same level as the second floor of the building. The range for this measurement is $70m$.

For the remainder of the paper, we define SINR to be equivalent to the modulation error ratio (MER). The true complex symbols sent by the transmitter are denoted by I_1+jQ_1, I_2+jQ_2, ... ,I_n+jQ_n. At the receiver, after channel equalization for amplitude, phase, and frequency offset, the decoded symbols are $\hat{I}_1 + j\hat{Q}_1$, $\hat{I}_2 + j\hat{Q}_2$, ... , $\hat{I}_n + j\hat{Q}_n$. MER is defined as

$$MER = \frac{\sum_{l=1}^{n}[I_l^2 + Q_l^2]}{\sum_{l=1}^{n}[(\hat{I}_l - I_l)^2 + (\hat{Q}_l - Q_l)^2]}. \quad (1)$$

In general, $\hat{I}_l + j\hat{Q}_l \neq I_l + jQ_l$ due to additive noise, interference, and non-perfect equalization. The first two are genuine aspects of SINR, while the third is an undesirable artifact whose effect on SINR computation we minimize by employing a large number of training symbols.

C. Transmitter and Receiver Software

The transmitter processing is as follows. Data symbols from a constellation of choice (e.g., M-QAM for $M = 16, 64, 256$) are randomly generated. The spreading code is applied, and a preamble is prefixed to each group of 120 coded data symbols. The entire packet is passed through an interpolating root-raised cosine filter with interpolation factor of 8. This defines a single transmitted packet for one user. One block of data consists of 500 distinct packets which are transmitted repeatedly in succession. The entire procedure is the same for the other users, with the only change being that a different LS code is used and different random data symbols are transmitted for each user. At the receiver, each block of complex symbols is processed separately. Within this block, the incoming data stream is match filtered to the root-raised cosine pulse. Standard algorithms for frequency offset, phase offset, and attenuation compensation are used (based on the known preamble symbols). We assume that frequency offset is block-wise constant (an assumption we have found true for blocks whose time duration is less than .1 second). The symbol error rate for a given packet is found by comparing the received symbols to the symbols known to have been sent by the transmitter for that packet. Since packets are transmitted in succession, a packet loss can be detected since the receiver finds a break in the expected packet sequence.

TABLE I
MEASUREMENT SCENARIOS AS SHOWN IN FIGURE 4.

Scenario	Tx_1 pos.	Tx_2 pos.	Rx pos.	Channel
1	P_1 to P_4	P_5	P_7	Indoor-to-Outdoor
2	P_{11}	P_{12} to P_{15}	P_{10}	Indoor-to-indoor
3	P_6	P_8	P_9	through-building

V. EXPERIMENTAL RESULTS

In this section, experimental results are presented based on the scenarios described in the previous section. We study performance of the approach in the presence of synchronization imperfections (both time and frequency) and interference for different M-QAM constellations. In addition, we experimentally illustrate the channel time and spatial coherence at low frequencies and its corresponding effect on the predictability of the power of the signal of interest and the interference, both measured at the intended receiver.

A. Experimental Results: Channel Spatial and Time Variation

As alluded to earlier, one way to exploit the low VHF channel is using higher order constellations which have better spectral efficiency; this is especially attractive for low frequency applications because the bandwidth of small antennas is relatively small. Furthermore, good time/spatial coherence properties of low VHF inspires the use of higher-order constellations since they inherently have increased coherence requirements. Here, we investigate the performance of our proposed approach for M-QAM (for M = 16, 64 and 256) in complex NLoS channels. We further introduce various levels imperfections including coarse synchrony and frequency offset (which we study via induced delays and frequency offsets among transmitters). We study the interference rejection in the presence of a moving interferer close to the receiver (i.e. the near-far problem) and quantify the effect of spatial and time variation on the received SINR of the user of interest in the presence of an interferer with higher power. The scenarios considered are described in Table I and Figure 4.

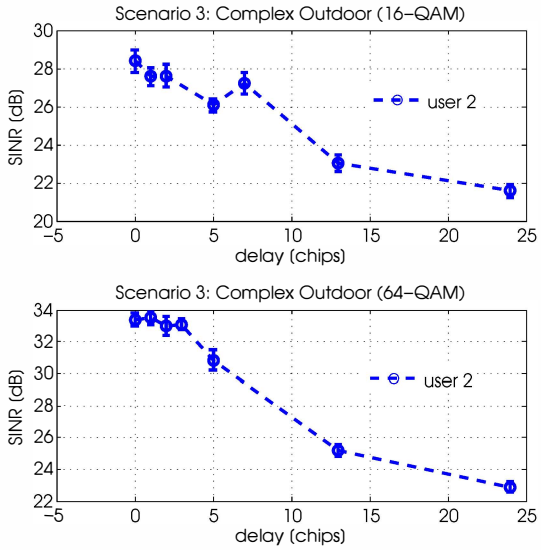

Fig. 5. The SINR measured for the user of interest (transmitter 2) is plotted vs delay in chips ($6.4\mu s$) for 16-QAM and 64-QAM. This measurement was performed in Scenario 3 where transmitter 2 and transmitter 1 were located at P_6 and P_8, respectively and the receiver is positioned at P_9 (see Table I). Even in this complex channel, the SINR variation within the ZCZ is minimal and significant degradation is seen outside the ZCZ.

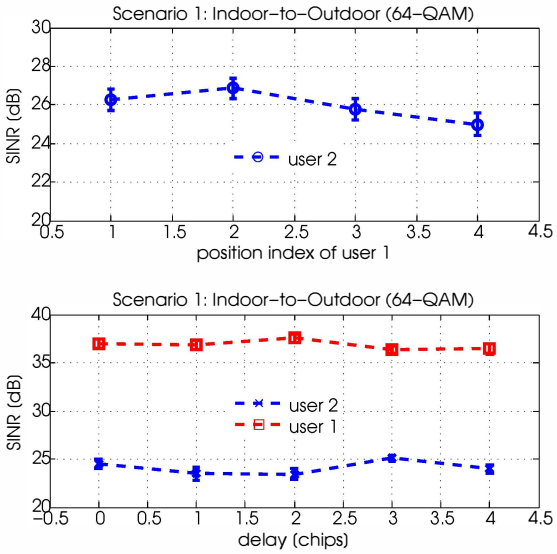

Fig. 6. The SINR measured for transmitter 2 (indoor) for various positions of transmitter 1 (interferer near the receiver) is shown in the top plot. The transmitter 2 was kept at the same location. The SINR vs delay (for both users) is also shown in the bottom plot for the same scenario.

The results in Figure 5 show experiments carried out in scenario 3 (through-building). The results show the SINR as a function of delay both within and outside the ZCZ. When the relative delays between users is within the ZCZ, the SINR is within 1.5 dB. These measurements illustrate that the SINR of the intended user (user 2 in this case) is minimally affected by interferer at various synchronization levels within the ZCZ for 16-QAM and 64-QAM. Outside, the ZCZ significant SINR degradation is observed in both cases.

In Figure 6, measurement results are shown for experiments

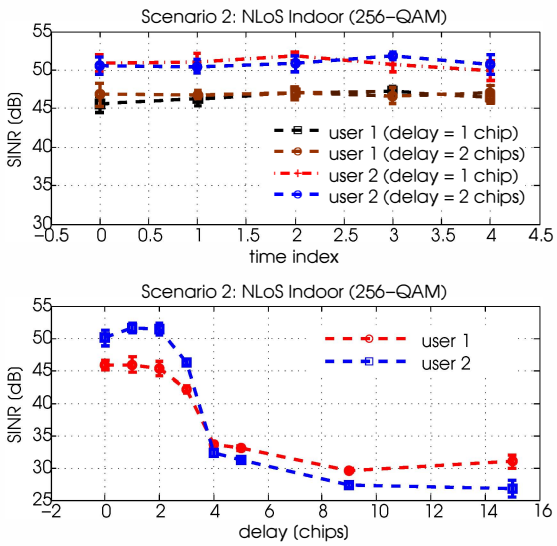

Fig. 7. In the bottom plot, the SINR measured for transmitter 1 and transmitter 2 versus delay of $6.4\mu s$ chips is shown for Scenario 2 where transmitter 2 and transmitter 1 are located at P_{15} and P_{11}, respectively (see Table I). The delay shown is the induced delay of transmitter 2 relative to transmitter 1. In order to study the performance of the proposed approach that leverages the time invariant characteristics of the channel, we perform various data collects at different time steps.The top plot shows the SINR vs time (for various collects) when both users are stationary. Here, a maximum variation in SINR of less than 1 dB is observed.

performed in scenario 1, where the receiver is positioned outside a five story building at P_7; transmitter 1 is moved near the receiver (P_1 to P_4) and transmitter 2 is positioned at the same location inside the first floor of the building $40m$ from the receiver at P_9 (see Table I). In the top plot of Figure 6, the SINR measured for transmitter 2 for various positions of transmitter 1 (interferer near the receiver) for 64-QAM is shown. It can be seen that transmitter 2's SINR variation for various position of the interferer is less than 1.5 dB. The bottom plot in Figure 6 shows SINR vs delay (within ZCZ) for scenario 1 for both users. This experimental result shows that coarse inter-user synchrony within ZCZ doesn't result in reduced SINR.

Next, we consider an indoor-to-indoor channel (scenario 2) consisting of offices and laboratories with large metallic partitions described in Table I. Figure 7 shows the variation of SINR as a function of delay as well as time for 256-QAM. As noted before, an advantage of low frequency operation is better channel coherence time as a result of reduced susceptibility to small scale fading effects (e.g., because of moving scatterers in indoor type environments) due to the relatively large wavelength. We study this aspect by acquiring data at different times for fixed positions of transmitters and the receiver. Specifically, we collect data five times (each collect is 0.5 second long) and the time interval between the different data collects is 10 seconds. The top plot in Figure 7 shows the SINR as a function of time (for various data collects and inter-user delays), when both users are stationary. This result shows that there is a maximum variation of 1.4 dB in SINR over a time scale of 50 seconds. The bottom plot shows SINR vs delay for both users which shows very minimal variation for

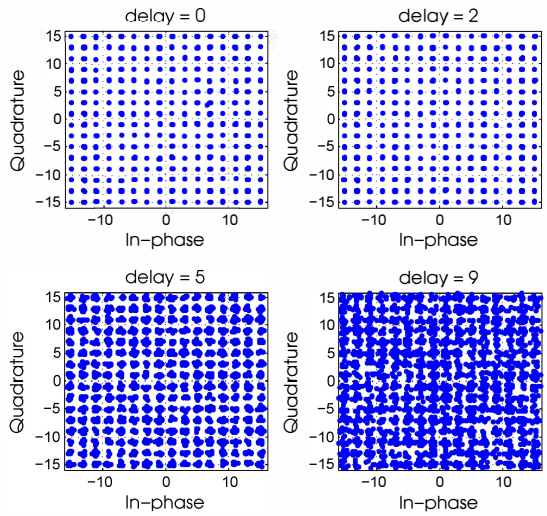

Fig. 8. The constellation diagram for a 256-QAM experiment versus known relative to delays (between users) within the ZCZ and outside of the ZCZ in chips. The experiment is carried out in Scenario 2 where transmitter 2 and user 1 are located at P_{15} and P_{11}, respectively (see Table I). The constellations are much tighter for delays within the ZCZ compared to those outside ZCZ since interference rejection is very high when the relative delays are within the ZCZ. The computed SINR for delays within ZCZ is 51 dB. At delay 5 and 9 chips, the SINRs are 31 and 27 dB, respectively. It should be noted that depending on the cross correlation profile of the codes considered, the SINR will vary significantly for different delays outside the ZCZ. For some delays outside the ZCZ, the symbol error rate will be much higher.

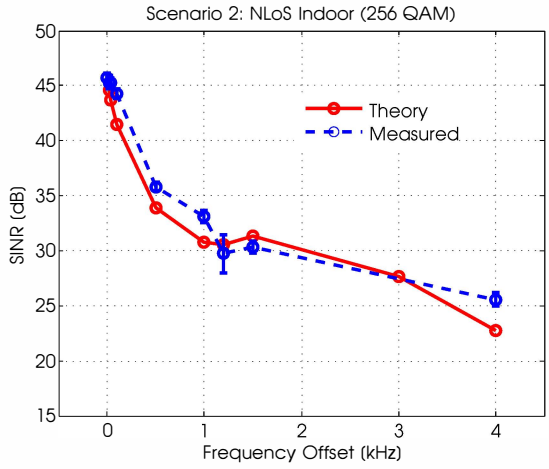

Fig. 9. In order to study the performance of the proposed approach as a function of frequency offset, we induce frequency offset in the carrier frequency of the interferer (transmitter 1) and carry out experiments in Scenario 2. The SINR computed for transmitter 2 versus frequency offset induced on the interferer (relative to transmitter 1) is shown. Small variation is observed for frequency offsets of 10s of Hz and the performance starts to degrade significantly for higher frequency offsets (100s of Hz).

inter-user delays that are within ZCZ and SINR degradation outside the ZCZ. Figure 8 shows measured constellations for the same setup as above. It is clear that the constellations are much tighter for delays within the ZCZ compared to those outside, since there is effectively a complete interference rejection within the ZCZ. We have also done experiments (results not shown) where the power of the interferer is up to 60 dB greater than the received power of the user of interest; in such cases, there is a minimal impact within the ZCZ, but the user of interest is undetectable outside.

B. Experimental Results: Frequency Offset Analysis

Here we illustrate the effect of frequency offset on performance. Frequency offsets on the order of 1 kHz are common at microwave frequencies. This frequency offset arises from the slight deviations in oscillators which are on the order of 1 part per million (ppm). Higher center frequencies thus have larger absolute deviations.

We perform an experiment to quantify SINR degradation as a function of inter-user frequency offsets of up to 4 kHz and compare against a theoretical frequency offset curve for the QS-DS-CDMA parameters from Section II. The theoretical frequency offset curve is generated as follows. For various frequency offsets f, we compute the lag 0 cross correlation between codes for transmitter 1 and transmitter 2, the latter of which is multiplied by a complex exponential of frequency f. The magnitude of this cross correlation, normalized by the magnitude of code 1, is computed, and defines a measure of interference. In order to generate the theoretical curve, we need a measure of system noise (to compute SINR in the 0 frequency offset case in the absence of interference). We estimate this from the experimental frequency offset curve by considering the SINR at 0 frequency offset based on which we estimate the system noise. Likewise, there is a power imbalance between the two transmitters due to using different amplifiers is compensated.

Figure 9 shows that the measured and theoretical results match well. The SINR of the user of interest varies within 4 dB for frequency offsets up to 100 Hz and then degrades significantly for higher frequency offsets. It should be noted that even at a frequency offset of 500 Hz, the SINR loss is about 10 dB. Note that these results are relative to bandwidth; a shorter chip time means the same frequency offset has less of an effect.

VI. Conclusion

In this paper, we have proposed a paradigm for multiuser communications among near ground mobile ad-hoc nodes in cluttered scenes. We have shown that the approach works well even with coarse time/frequency/power synchrony. Our approach leverages the QS-DS-CDMA paradigm along with the favorable propagation characteristics of the lower VHF band. This work illustrates that QS-DS-CDMA coupled with lower VHF enjoys LoS-like performance even in near-ground NLoS scenarios that pose significant challenges to microwave frequencies.

Based on simulations as well as experiments carried out in three different scenarios in and around a large 5 story building, we illustrate that we can achieve very low MAI even in the presence of the near-far effect. We also illustrate the performance loss outside the ZCZ, which is dependent on the inter-user delay. The effect of frequency offset on the performance of the proposed approach is also studied experimentally, and we show that the effects at lower VHF are minimal for frequency offsets that are present in the example system described in Section II.

There are several interesting directions in which this work can be extended. We have demonstrated the spatial and temporal stability of the SINR of the signal of interest within the ZCZ. The large coherence scales suggest that the rate of training/preamble symbols for channel estimation can be markedly reduced. In this paper, we have not explicitly commented on the mechanism ensuring time synchronization. This may be accomplished by intermittent GPS access; alternatively, one may consider the use of a lower VHF beacon node which (exploiting excellent penetration) provides a time reference to all other nodes. If the time-delay tolerance between nodes is to be relaxed, one may consider using QS-DS-CDMA with multiple carriers; the use of more carriers increases the effective chip time and hence the time duration of the ZCZ.

REFERENCES

[1] F. T. Dagefu, G. Verma, C. Rao, P. Yu, J. R. Fink, B. M. Sadler, K. Sarabandi, "Short-range low-VHF channel characterization in cluttered environments," *IEEE Trans. Ant. & Propag.*, vol. 63, no. 6, June 2015.

[2] F. T. Dagefu, J. Choi, M. Sheikhsofla, B. M. Sadler and K. Sarabandi, "Performance Assessment of Lower VHF Band for Short Range Communication and Geolocation Applications", *Radio Science,* April 2015.

[3] S. M. Moon, H. K. Ryu, J. M. Woo, H. Ling, "Miniaturisation of $\lambda/4$ microstrip antenna using perturbation effect and plate loading for low-VHF-band applications," *Electronics Letters*, vol.47, no.3, Feb. 2011.

[4] J. Oh, J. Choi, F. T. Dagefu, K. Sarabandi, "Extremely small two-element monopole antenna for HF band applications," *IEEE Trans. Ant. & Propag.*, vol. 61, pp: 2991 - 2999, no. 6, June 2013.

[5] J. Choi, F. T. Dagefu, B. M. Sadler and K. Sarabandi "Electrically small folded dipole antenna for HF and VHF bands," *IEEE Trans. Ant. & Wireless Propag. Letters* (to appear).

[6] S. Zhao, C. Fumeaux and C. Coleman, "Miniaturised high-frequency and very-high-frequency antennas based on optimized non-uniform helical structures," *Microwaves, Antennas & Propagation, IET*, vol.6, no.6, April 24 2012.

[7] S. Lim, R. L. Rogers; H. Ling, "A tunable electrically small antenna for ground wave transmission," *IEEE Trans. Ant. & Propag.*, vol.54, no.2, Feb. 2006.

[8] F. T. Dagefu, J. Oh and K. Sarabandi,"A sub-wavelength RF source tracking system for GPS-denied environments," *IEEE Trans. on Ant. & Prop.*, vol. 61, no. 4, April 2013.

[9] J. Andrusenko, R. L. Miller, J. A. Abrahamson, N. M. Merheb Emanuelli, R. S. Pattay and R. M. Shuford, "VHF general urban path loss model for short range ground-to-ground communication", *IEEE Trans. on Ant. & Prop.*, vol. 56, no. 10, October 2008.

[10] G. Verma, F. T. Dagefu, B. M. Sadler, and K. Sarabandi,"Direction of arrival estimation with the received signal strength gradient at the lower VHF band," *IEEE Int. Symp. Ant. & Prop., Fajardo, PR, 2016*.

[11] F. T. Dagefu and K. Sarabandi, "Analysis and Modeling of Near-ground Wave Propagation in the Presence of Building Walls," *IEEE Trans. on Ant. & Prop.*, vol. 59, no. 6, pp. 2368-2378, June 2011.

[12] D. Liao, K. Sarabandi,"Near-Earth wave propagation characteristics of electric dipole in presence of vegetation or snow layer," *IEEE Trans. Ant. & Propag.*, vol.53, no.11, pp.3747-3756, Nov. 2005.

[13] V. M. DaSilva and E. S. Sousa, "Multicarrier orthogonal CDMA signals for quasi-synchronous communication systems," *IEEE Journal on Selected Areas in Communications*, vol. 12, no. 5, pp. 842–852, 1994.

[14] P. Z. Fan, "Spreading sequence design and theoretical limits for quasisynchronous CDMA systems," *EURASIP J. Wireless Comm. and Networking*, vol. 2004, no. 1, pp. 19–31, 2004.

[15] K. W. Yip and T. S. Ng, "Effects of carrier frequency accuracy on quasi-synchronous, multicarrier DS-CDMA communications using optimized sequences," *IEEE Journal on Selected Areas in Communications*, vol. 17, no. 11, pp. 1915–1923, 1999.

[16] G. Verma, F. T. Dagefu, B. M. Sadler, and P. Spasojevic,"Implications of Time/Frequency Synchronization Tradeoff of Multi-carrier Quasi-Synchronous DS-CDMA for Robust Communications at Lower VHF," *MILCOM, Baltimore, MD, 2016*.

[17] J. Omura, "Spread spectrum communications handbook," *vol. 2. McGraw-Hill, 1994*.

[18] S. Willenegger, "CDMA2000 physical layer: An overview,"*Journal of Communications and Networks*, vol. 2, no. 1, pp.5-17.

[19] P.Z. Fan, N. Suehiro, N. Kuroyanagi, X. M. Deng. "Class of binary sequences with zero correlation zone." *Electronics Letters*, vol. 35 no. 10, pp. 777-779, 1999.

[20] K. Bonna, E. Kanterakis, W. Su, T. M. Ryder and P. Spasojevic, "Distributed RF sensing using software-defined radios," *49th Annual Conference on Information Sciences and Systems (CISS)*, pp. 1-5, Baltimore, MD, 2015.